



**HAL**  
open science

## **New clinicopathological associations and histoprognostic markers in ILAE types of hippocampal sclerosis**

Ana Laura Calderon-Garcidueñas, Bertrand Mathon, Pierre Lévy, Anne Bertrand, Karima Mokhtari, Séverine Samson, Valérie Thuriès, Virginie Lambrecq, Vi-Huong Nguyen-Michel, Sophie Dupont, et al.

### ► **To cite this version:**

Ana Laura Calderon-Garcidueñas, Bertrand Mathon, Pierre Lévy, Anne Bertrand, Karima Mokhtari, et al.. New clinicopathological associations and histoprognostic markers in ILAE types of hippocampal sclerosis. *Brain Pathology*, 2018, 10.1111/bpa.12596 . hal-01730593

**HAL Id: hal-01730593**

**<https://hal.sorbonne-universite.fr/hal-01730593v1>**


Submitted on 13 Mar 2018

**HAL** is a multi-disciplinary open access archive for the deposit and dissemination of scientific research documents, whether they are published or not. The documents may come from teaching and research institutions in France or abroad, or from public or private research centers.

L'archive ouverte pluridisciplinaire **HAL**, est destinée au dépôt et à la diffusion de documents scientifiques de niveau recherche, publiés ou non, émanant des établissements d'enseignement et de recherche français ou étrangers, des laboratoires publics ou privés.

# New clinicopathological associations and histoprognostic markers in ILAE types of hippocampal sclerosis

## Authors:

Ana Laura Calderon-Garcidueñas<sup>1,2</sup>, Bertrand Mathon<sup>3,5</sup>, Pierre Lévy<sup>4,5</sup>, Anne Bertrand<sup>5,6,7,8</sup>, Karima Mokhtari<sup>1,6</sup>, Séverine Samson<sup>9</sup>, Valérie Thuriès<sup>1</sup>, Virginie Lambrecq<sup>9,5,6</sup>, Vi-Huong Nguyen-Michel<sup>9</sup>, Sophie Dupont<sup>9,5,6,10</sup>, Claude Adam<sup>9,6</sup>, Michel Baulac<sup>9,5,6</sup>, Stéphane Clémenceau<sup>3</sup>, Charles Duyckaerts<sup>1,5,6</sup>, Vincent Navarro<sup>9,5,6</sup>, Franck Bielle<sup>1,5,6</sup> 

## Affiliations:

1 AP-HP, Hôpitaux Universitaires Pitié-Salpêtrière Charles Foix, Department of Neuropathology, Paris, France

2 Institute of Forensic Medicine, Universidad Veracruzana, Boca del Río, Mexico

3 AP-HP, Hôpitaux Universitaires Pitié-Salpêtrière Charles Foix, Department of Neurosurgery, Paris, France

4 UPMC and Inserm UMR S 1136 (EPAR team), Département de Santé Publique, Hôpital Tenon, Groupe Hospitalier Universitaire de l'Est Parisien, AP-HP, Paris, France

5 Sorbonne University, UPMC, Univ Paris 06, Paris, France

6 Brain and Spine Institute (ICM; INSERM, UMRS 1127; CNRS, UMR 7225), Paris, France

7 Inria Paris, Aramis project-team, Paris, France

8 AP-HP, Hôpital Saint Antoine, Department of Radiology, Paris, France

9 AP-HP, Hôpitaux Universitaires Pitié-Salpêtrière Charles Foix, Department of Epileptology, Paris, France

10 AP-HP, Hôpitaux Universitaires Pitié-Salpêtrière Charles Foix, Department of Rehabilitation, Paris, France

## Corresponding authote

Franck Bielle

Service de Neuropathologie du Pr Duyckaerts

Laboratoire Escourolle

Hôpital de la Pitié-Salpêtrière

47-83 Bd de l'Hôpital

75651 PARIS CEDEX 13

[franck.bielle@aphp.fr](mailto:franck.bielle@aphp.fr)

This article has been accepted for publication and undergone full peer review but has not been through the copyediting, typesetting, pagination and proofreading process which may lead to differences between this version and the Version of Record. Please cite this article as an 'Accepted Article', doi: 10.1111/bpa.12596

Tel: +33 1 42 16 18 90

Fax: +33 1 42 16 18 99

### **Running title**

Classification of hippocampal sclerosis

### **Acknowledgments**

We are grateful to to Béatrice Bonneau, Léna Gernez and Andry Ralitera for the technical assistance.

### **Fundings**

The work of FB is supported by a grant from Fondation ARC pour la recherche sur le cancer (PJA 20151203562).

The authors declare no conflict of interest.

Accepted Article

## Abstract

Mesial temporal lobe epilepsy with hippocampal sclerosis (MTLE-HS) is a heterogeneous syndrome. Surgery results in seizure freedom for most pharmacoresistant patients, but the epileptic and cognitive prognosis remains variable. The 2013 International League Against Epilepsy (ILAE) histopathological classification of hippocampal sclerosis (HS) has fostered research to understand MTLE-HS heterogeneity. We investigated the associations between histopathological features (ILAE types, hypertrophic CA4 neurons, granule cell layer alterations, CD34 immunopositive cells) and clinical features (presurgical history, postsurgical outcome) in a monocentric series of 247 MTLE-HS patients treated by surgery. NeuN, GFAP and CD34 immunostainings and a double independent pathological examination were performed. 186 samples were type 1, 47 type 2, 7 type 3 and 7 samples were gliosis only but no neuronal loss (noHS).. In the type 1, hypertrophic CA4 neurons were associated with a worse postsurgical outcome and granule cell layer duplication was associated with generalized seizures and episodes of status epilepticus. In the type 2, granule cell layer duplication was associated with generalized seizures. CD34+ stellate cells were more frequent in the type 2, type 3 and in noHS. These cells had a Nestin and SOX2 positive, immature neural immunophenotype. Patients with nodules of CD34+ cells had more frequent dysmnestic auras. CD34+ stellate cells in scarce pattern were associated with higher ratio of normal MRI and of stereo-electroencephalographic studies. CD34+ cells were associated with a trend for a better postsurgical outcome. Among CD34+ cases, we proposed a new entity of BRAF V600E positive HS and we described three hippocampal multinodular and vacuolating neuronal tumours. To conclude, our data identified new clinicopathological associations with ILAE types. They showed the prognostic value of CA4 hypertrophic neurons. They highlighted CD34+ stellate cells and BRAF V600E as biomarkers to further decipher MTLE-HS heterogeneity.

**Key words:** epilepsy; hippocampal sclerosis; ILAE classification; CD34; hypertrophy

## INTRODUCTION

Mesial temporal lobe epilepsy with hippocampal sclerosis (MTLE-HS) is often resistant to anti-epileptic drugs (32). Epilepsy surgery results in a decrease in the frequency of the seizures or in their cessation in

most cases of pharmaco-resistant MTLE-HS. In some patients, however, epilepsy may recur after surgery and cognitive impairments, especially memory deficits, may be observed (15, 46). The uncertainty of postoperative prognosis makes difficult the decision to operate upon a case of MTLE-HS. A better understanding of the histopathological heterogeneity and of its effects on seizure frequency and cognitive outcome after surgery is needed.

Clinical studies describe a variable aetiology and history for MTLE-HS patients (17, 45). The natural history often begins with an initial precipitating injury (IPI). IPIs in infancy –most frequently febrile seizures (FS)- are considered causative for MTLE-HS (13). Spontaneous seizures occur after a latent period. Tumours or focal cortical dysplasias/FCD may also induce HS and MTLE (18).

The neuropathology of HS is heterogeneous. There are diverse patterns of neuronal loss, gliosis and changes in the granule cell layer (GCL) which have been linked to surgical outcomes (15). Several classifications have been proposed (47). An international consensus reached in 2013 (4, 5, 9, 40) defined three patterns of HS (type 1 with severe neuronal loss in CA1 and CA4, type 2 with predominant loss in CA1, type 3 with predominant loss in CA4) and a pattern “noHS, gliosis only” without neuronal loss. Type 1 is the most frequent and typical aspect with most severe neuronal loss in the Ammon horn, dense gliosis, GCL dispersion and often CA4 neurons with increased size. Such CA4 neurons were previously described as “hypertrophic neurons” by Thom et al (38, 39). However, the ILAE Diagnostic Methods Commission established a consensual definition of “hypertrophic neuron” in the context of FCD (6) but not in the context of HS (5). The term “CA4 hypertrophic neurons” here refers to CA4 pyramidal neurons with increased size of the cell soma and nucleus.

CD34 immunopositive (CD34+) multipolar or stellate cells have been described in distinct forms of epilepsy-related cerebral lesions including ganglioglioma, dysembryoplastic neuroepithelial tumours (DNET) (2, 29), multinodular and vacuolating neuronal tumours (MVNT) (16, 41) and FCD (10, 23). The nosology of lesions containing these CD34+ cells without another specific tumoral component is not consensual and they are interpreted by some authors as the periphery of a ganglioglioma or as a non-specific/diffuse form of DNET (43). In this context, we preferred to use a descriptive definition of nodules of CD34+ stellate cells and of scarce CD34+ stellate cells. CD34+ cells express the intermediate filament Nestin but not Glial Fibrillary Acidic Protein, (GFAP) – a pattern reminiscent of the phenotype of immature neural cells (43). The tumoral, dysplastic or reactive nature of CD34+ cells in samples of epilepsy surgery remains debated and their contribution to the nosology of MTLE-HS is not known.

We investigated clinicopathological correlations using the ILAE classification of HS types and of the pattern no HS in a monocentric series of 247 patients undergoing surgery for MTLE-HS including hippocampus resection. We characterized the CD34+ cells in these lesions in order to enhance the nosology of MTLE-HS. We previously reported that ILAE types did not have prognostic value for the post-surgical outcome of epilepsy in this cohort (25). We tested if the histopathological features associated with ILAE types might have a prognostic value.

## **MATERIAL AND METHODS**

### **Patients and samples**

The histopathological features of hippocampectomy samples of all adult patients (i) with MTLE-HS (ii) treated with surgery at the Pitié-Salpêtrière Hospital between 1995 and 2015, and (iii) with available histological material were analyzed (Supplemental Figure 1). Surgical samples of hippocampal tumors, glial scars, vascular malformations were excluded. Three surgical approaches were used: anterior temporal lobectomy (ATL, n=127), transcortical selective amygdalohippocampectomy (n=114) and transylvian selective amygdalohippocampectomy (n=6) (25). The procedures taken to protect personal data in this work were approved by the French National Technologies and Civil Liberties Commission. Collected data included age, gender, medical history, seizure types, surface, and when performed, intracranial EEG records, presurgical neurological and cognitive status, presurgical anti-epileptic treatment, and postsurgical outcome. No history of limbic encephalitis was noted. MRI findings were reviewed by a neuroradiologist (AB) for MVNT and “BRAF V600E+ HS” as defined hereafter.

### **Pathology**

Hippocampal samples were examined microscopically after hematoxylin and eosin staining and immunostaining for GFAP and NeuN.. Temporal lobe was examined in patients treated by ATL. Samples were included only when CA1 and CA4 hippocampal subfields could be evaluated. Samples lacking CA1 or CA4 and fragmented samples were excluded (Supplemental Figure 1). The anatomic definition of CA1, CA2, CA3 and CA4 was as defined previously (5). The diagnosis of tumors was defined by WHO 2016 (22). FCD was classified as previously defined (6). Two neuropathologists (FB and ALCG) separately attributed each sample to

a ILAE type of HS (5), and reviewed slides together, using a multi-head microscope, so that a consensus conclusion could be agreed if initial classifications diverged. Unresolved cases were reviewed by a third neuropathologist (CD).

The neuronal loss in CA1, CA2, CA3, CA4 and in the GCL was evaluated semi-quantitatively from 0% to 100% by 10% increments in comparison with controls. As controls, postmortem samples of hippocampus from patients without neurological symptoms and without brain lesion were used. Consent was obtained from the legally authorized family members. Changes in the distribution of granule cells were grouped under two subheadings: “dispersion” when the layer was more than 10 neurons thick (45) and “duplication” when two layers could be readily distinguished. “Broadening” of the GCL means both “dispersion” or “duplication”. When both dispersion and duplication were present, the sample was classified in the duplication subgroup. We also took note of CA4 hypertrophic neurons.

### **Immunohistochemistry**

Formalin-fixed paraffin-embedded tissue sections (3 µm of thickness) were deparaffinized and immunolabelled with a Ventana Benchmark XT stainer (Roche, Basel, Switzerland). The secondary antibodies were coupled to peroxidase with diaminobenzidine as brown chromogen or to alkaline phosphatase with Fast Red (ultraView Universal Alkaline Phosphatase Red Detection Kit, VentanaVR) as red chromogen. Primary antibodies were as follows: BRAF V600E (mouse monoclonal VE1, 1:100, Abcys Eurobio), CD31 (monoclonal mouse JC70A, 1:30, Dako) CD34 (monoclonal mouse QBEnd10, 1:50, Dako), ELAVL2 (rabbit polyclonal, 1:500, Proteintech), GFAP (monoclonal mouse 6F2, 1:500, Dako), Internexin alpha/INA (monoclonal mouse 2E3, 1:100, Quartett Biochemicals), Nestin (monoclonal mouse 10C2, 1:2000, Sigma-Aldrich), NeuN (Monoclonal mouse MAB377, 1:100; Merck Millipore), OLIG2 (rabbit monoclonal EP112, 1:200, Epitomics), P53 (monoclonal mouse, DO-7, 1:100 Dako), SOX2 (rabbit monoclonal SP76, 1:300, Sigma-Aldrich), Vimentin (monoclonal mouse V9, 1:50 Dako). The quality of immunolabelings was assessed by an external positive control for BRAF V600E (a BRAF V600E mutant colic adenocarcinoma was added on each slide) and P53 (an IDH mutant and P53 mutant anaplastic astrocytoma was processed on another slide). The quality was assessed by internal positive controls for the other antibodies. The CD34 immunolabeling was unsuccessful in 8 cases (Supplemental Figure 1). It was tested only on the hippocampus, the extra hippocampal region was not tested in cases of ATL. CD34 immunolabeling was classed as “CD34-” if only endothelial cells were positive, as “CD34+ scarce” if only a few

isolated extravascular stellate cells were detected, or as CD34+ nodular if the extravascular stellate cells detected were grouped in nodules in the hippocampus. We further characterized all “CD34+ nodular” samples (n=8) and a subset of “CD34+ scarce” samples (n=11) by BRAF V600E, P53, INA, and ELAVL2 immunolabelings.

### **Statistical Analysis**

Quantitative variables are shown as mean±standard deviation. The nominal variables were tested with chi-squared test or exact test of Fisher when appropriate. Continuous variables were tested by Kruskal-Wallis test for 3 groups, the Mann-Whitney test for 2 groups and the t test when variable was normally distributed. Spearman’s correlation coefficient was used to test the correlation of continuous variables. The postsurgical outcome was evaluated by Kaplan-Meier plots for the Engel I and Ia classes across time. Differences of outcome were assessed by the log-rank test. The significance level was on-adjusted  $p < 0.05$ , two sided test. Statistical analysis was performed with the software StatView 5.0.

## **RESULTS**

### *General features of the whole series*

Our series included 247 patients with mean age at surgery of  $38.2 \pm 10.9$  years and gender ratio of 1:1. Its features are summarized in Table 1 and Supplemental Table 1. The mean age at epilepsy onset and the mean duration of epilepsy were  $12.3 \pm 9.3$  years and  $26.0 \pm 11.7$  years, respectively. Both parameters were distributed unimodally (Supplemental Figure 1). The mean duration of epilepsy was stable across time ( $\rho=0.08$   $p=0.22$ ).

### *Histopathological correlates of ILAE types*

ILAE type 1 was found in 75% of cases. ILAE types 2, 3 and the pattern noHS were present in 19%, 3% and 3% of the samples respectively (Table 2, Supplemental Table 2). The kappa coefficient testing the inter-observer reproducibility of ILAE type assessment was 0.612 (generally considered as “substantial” agreement). The distribution of neuronal loss across ILAE types was similar to the previously reported one (Supplemental Figure 2). The size of CA4 hypertrophic neurons was significantly increased compared to CA4 pyramidal neurons of a control hippocampus (Supplemental Figure 3). CA4 hypertrophic neurons were detected more often in type 1 than in either type 2, 3 or noHS (type 1: 57%, type 2: 15%, type 3: 14%, noHS: 0%  $p=2 \times 10^{-7}$ , Table 2). In type 1, CA4 hypertrophic neurons were associated with higher neuronal loss in CA1 ( $p=0.047$ ). One dysplasia



was observed in a type 3 HS patient and corresponded to an increased density of neurons in CA3 associated with abnormal ganglionic aspect of neurons and abnormal astrocytic cells.

#### *Histopathological correlates of granule cell layer alterations*

The GCL was classified as of normal width (23%), dispersed (66%) or duplicated (10%, Table 3, Supplemental Table 3, Supplemental Figure 3). The GCL was significantly more likely to be dispersed or duplicated in type 1 than in noHS (type 1 81%, no HS 2/7 29%,  $p=0.005$ ). GCL dispersion was associated with higher neuronal loss in the CA2 and CA3 fields ( $p=0.045$  and  $p=0.003$  respectively). GCL broadening was associated with higher neuronal loss in the CA4 field ( $p=0.003$ ).

#### *Histopathological correlates of CD34 immunoreactive stellate cells*

Three patterns were recognized: “CD34-”, “CD34+ scarce”, and “CD34+ nodular” (Table 4, Supplemental Table 4, Figure 1). The CD34+ cells presented ramified cytoplasmic processes with a stellate aspect. The nucleus had slight anisokaryosis and nuclear membrane irregularities. Nestin immunolabeling was positive in endothelial cells but also revealed a stellate pattern in areas with CD34+ stellate cells ( $n_{\text{CD34+ nodular}}=7$ ,  $n_{\text{CD34+scarce}}=10$ ). Co-immunolabeling confirmed a co-expression of Nestin and CD34 by stellate cells ( $n_{\text{CD34+ nodular}}=4$ ,  $n_{\text{CD34+scarce}}=3$ ). No stellate pattern was observed with Vimentin ( $n_{\text{CD34+ nodular}}=7$ ,  $n_{\text{CD34+scarce}}=11$  Figure 1) nor CD31 ( $n_{\text{CD34+ nodular}}=5$ ,  $n_{\text{CD34+scarce}}=7$  data not shown) whereas both markers are expressed by endothelial cells. Co-immunolabeling showed a co-expression of CD34 and SOX2 in some CD34+ stellate cells ( $n=3$  Figure 2) whereas SOX2 was negative in endothelial cells ( $n=19$ ). Co-immunolabeling showed a co-expression of CD34 and OLIG2 in some CD34+ stellate cells ( $n=3$  Supplemental Figure 4) whereas OLIG2 was negative in endothelial cells ( $n=10$ ). Together CD34+ stellate cells are Nestin+, SOX2+/-, OLIG2+/-, CD31-, Vimentin- and can be distinguished from endothelial cells that are CD34+, Nestin+, SOX2-, OLIG2-, CD31+, and Vimentin+.

One hundred and ninety six samples were “CD34-”, 35 were “CD34+ scarce” and 8 cases were “CD34+ nodular”. Samples with CD34+ stellate cells were significantly associated with type 2 (26%) and with noHS (71%) rather than with type 1 (13%,  $p=0.0002$ ). “CD34+ scarce” was associated with noHS (57%) compared to the type 1 (12%,  $p=0.004$ ). “CD34+ nodular” labeling was more frequently observed in the type 2 (7%,  $p=0.023$ ), in the type 3 (43%  $p=0.0002$ ) and in noHS samples (43%,  $p=0.0004$ ) rather than in the type 1 (0.6%).

BRAF V600E positive mononucleated neurons were observed in the CD34+ nodular group ( $n=3/8$ ), and in the CD34+ scarce group ( $n=2/11$ ): they were located in dentate gyrus, cornu ammonis and subiculum and were associated with P53 positive cells ( $n=4$ , Figure 1) but no ganglioglioma or DNET was found. These HS

(n=1 type 1, n=3 type 2, n=1 type 3) are further called “BRAF V600E+ HS”. By contrast, in three other CD34+ nodular samples, the neuronal markers INA and ELAVL2 were intensely positive in abnormal, ectopic and often vacuolated neurons in the white matter of the subiculum, alveus and fimbria whereas NeuN was negative in these cells (Figure 2, Supplemental Figure 4). These samples (n=2 type 3, n=1 noHS) were further considered as the hippocampal localization of MVNT. The BRAF V600E+ HS and hippocampal MVNT were mutually exclusive. They were not observed in CD34- samples ( $n_{\text{BRAF V600E}}=11$ ,  $n_{\text{INA}}=13$ ).

The MRI findings were available for two cases of BRAF V600E+ HS and showed a typical hippocampal sclerosis (Figure 3). They were available for two cases of hippocampal MVNT. They showed T2 and FLAIR hyperintensities involving hippocampus and extrahippocampal structures and a pseudocyst, and were compatible with a DNET or MVNT (Figure 3).

#### *Presurgical clinical correlates of ILAE types*

We analyzed relations between the different patterns of HS and the presurgical clinical data (Table 2, Supplemental Table 2).

In the type 1, most patients presented an IPI (77%) with a majority of FS (56%). In the type 1 with FS as IPI, CA2 neuronal loss was significantly positively correlated with the age at FS ( $n=69$ ,  $p=0.0035$ ,  $\rho=0.36$ , Supplemental Figure 1). In the type 2, patients presented the highest prevalence of IPI (89%) with a majority of FS ( $n=32/47$  68%). In the type 3, we noted no FS, a low prevalence of IPI (43%), and a trend for an older age of onset and at surgery ( $18.6 \pm 11.2$  and  $40.9 \pm 16.1$  respectively). In the pattern noHS, there were fewer IPI (33%  $p=0.001$ ), fewer FS (17%  $p=6 \times 10^{-4}$ ), and less abnormal MRI aspect (29%  $p=7 \times 10^{-8}$ ) compared to types 1 or 2. Stereo-electroencephalographic studies (sEEG) had been performed more frequently in noHS (71%) than type 1 (8%) and type 2 (2%  $p=6 \times 10^{-5}$ ). There was a trend for an older age at onset ( $17.3 \pm 10.0$ ) than in type 1 and 2. The duration of epilepsy was shorter in noHS than in types 1 and 2 but not at a level of significance ( $\text{duration}_{\text{type 1}}=26.0$  y;  $\text{duration}_{\text{type 2}}=26.6$  y;  $\text{duration}_{\text{type noHS}}=24.5$  y;  $p=0.64$ ).

We analyzed the relationships between different patterns of GCL alterations and the presurgical clinical data (Table 3, Supplemental Table 3). GCL broadening (i.e. dispersion or duplication) was more frequent in female patients (male 71%, female 82%,  $p=0.044$ ). GCL duplication was significantly associated with a history of status epilepticus (normal GCL 2%, dispersion 10%, duplication 20%,  $p=0.04$ ) and with the occurrence of generalized seizures (normal GCL 71%, dispersion 68%, duplication 96%,  $p=0.02$ ). Normal GCL pattern was associated with a normal MRI (normal GCL 10%, broadening 2%,  $p=0.04$ ).

We analyzed the relations between different CD34+ cells patterns and the presurgical clinical data (Table 4, Supplemental Table 4). The “CD34+ nodular” group presented more frequent dysmnestic auras (CD34- 34%; CD34+ scarce 43%; CD34+ nodular 88%;  $p=0.006$ ). In the “CD34+ scarce” group, sEEG had been more often performed (CD34- 7%; CD34+ scarce 20%; CD34+ nodular 13%;  $p=0.037$ ) and the MRI was more often normal (CD34- 2%; CD34+ scarce 13%; CD34+ nodular 0%;  $p=0.022$ ).

#### *Prognostic value of histopathological lesions*

In the type 1, CA4 hypertrophic neurons were predictive of a worse prognosis for Engel I ( $p=0.045$ ) and Engel Ia ( $p=0.0046$ ) (Figure 4). In the types 1 and 2, GCL dispersion and duplication had no prognostic value. The presence of CD34 stellate cells was associated with a trend for a better prognosis for the Engel Ia class ( $p=0.06$ ).

## **DISCUSSION**

Here we report correlations between clinical and pathological data in samples from a large monocentric series of MTLE patients with HS patterns classified according to ILAE guidelines. These data confirmed some previously reported correlations, and identified novel links between distinct forms of HS and the occurrence of histological lesions, CD34+ stellate cells, seizure symptoms, epilepsy severity and postsurgical outcome.

This series of pharmacoresistant MTLE patients had a similar mean age at epilepsy onset, a longer duration of epilepsy and an older age at surgery than for some previous reports. Supplemental Table 5 lists associations between clinical and pathological data confirmed in this study (3, 4, 11, 27, 37, 40). The good interobserver reproducibility of ILAE classification in our series and the confirmation of main previous findings from other teams strengthen the interest of this methodology in order to compare data between teams of epilepsy surgery. We included cases with analysable CA1 and CA4 because we can classify them into neuronal loss predominant in CA1 (type 2), in CA4 (type 3) or in both (type 1). CA2 and CA3 were not analysable in some cases, which could limit our conclusions because we cannot exclude that some of these cases have neuronal loss predominant in CA2 or CA3. However, ILAE classification does not define HS by predominant neuronal loss in CA2 or CA3 and we did not observe it in our large series. Although we evaluated neuronal loss only by a semi-quantitative visual evaluation, neuronal loss in CA2, CA3 and GCL, was more extreme for type 1 than type 2 and more severe for type 2 than noHS as reported (4). GCL dispersion or duplication was more frequent for type

1, and associated with a higher neuronal loss in CA4 as previously reported (3, 8, 24, 40, 42). We observed a trend for more IPI (including FS) in type 2, as did the study of Thom et al (40). We observed a trend for GCL dispersion in older patients, as previously reported (3). Samples with noHS were associated with shorter epilepsy duration, and less IPI (including FS). In a well-defined group of type 1 with FS, we found a positive correlation between age at IPI and CA2 neuronal loss: our data suggests that the survival of CA2 neurons is enhanced when an IPI occurs earlier.

Hypertrophic CA4 neurons were associated with type 1 and a higher neuronal loss in CA4 in our series as previously reported (7, 30, 38, 39). They are thought as an alteration induced by epilepsy rather than dysplastic neurons (7, 30). mTOR pathway activation in the dysmorphic neurons of tubers or FCD causes hypertrophy and epileptogenesis (19, 26). This activation can also be induced by epilepsy (33, 34) and was described in CA4 hypertrophic neurons of HS (21). We identified CA4 hypertrophic neurons as a new pejorative prognostic factor for postsurgical outcome in type 1. These abnormal neurons could be a biomarker of a more severe injury epilepsy and of mTOR activation. Further studies are required to decipher the pathophysiological role of CA4 hypertrophic neurons.

GCL broadening has been linked to seizures and suggested to reflect either newly generated neurons or abnormal somatic migration of mature granule cells (3, 38). We detected GCL broadening more frequently in female than in male patients. Gender-linked effects of estrogens on hippocampal neurogenesis have been described (1, 12, 35, 36). Estrogen modulates hippocampal neuronal networks in part via Brain Derived Neurotrophic Factor, a neurotrophin that increases granule cell neurogenesis, ectopic granule cells and transmission mediated by mossy fibers (14, 31, 44). Our data show that GCL duplication is associated with generalized seizures and status epilepticus, raising a possible link between this histological lesion and more severe epilepsies. Alternatively, generalized seizures may favour a dual layer of granule cell bodies.

We examined CD34<sup>+</sup> stellate cells. Their Nestin<sup>+</sup>, SOX2<sup>+/-</sup>, OLIG2<sup>+/-</sup>, CD31<sup>-</sup>, Vimentin<sup>-</sup> immunophenotype favors an immature neural cell type. We observed BRAF V600E positive neurons in three “CD34<sup>+</sup> nodular” and two “CD34<sup>+</sup> scarce” HS. As there was no radiological or histopathological evidence of tumours in these cases and as the predominant lesions were neuronal loss and gliosis, we named these cases “BRAF V600E<sup>+</sup> HS”. In vivo electroporation studies in the murine embryonic cortex showed that mild activation of Extracellular-signal-

regulated kinase/ERK signaling driven by BRAF V600E or Ras led to the production of abnormally specified neurons whereas strong activation of ERK signaling drives gliomagenesis (20). These observations open the intriguing hypothesis that the presence of a BRAF V600E mutation in a subset of hippocampal neurons could drive epilepsy without tumorigenesis. Among CD34+ cases, we described three cases of hippocampal MVNT. The tumoral or dysplastic etiology of this lesion is debated (16, 41). We confirmed the absence of BRAF V600E mutation and the CD34 and INA immunopositivity of MVNT (16, 28, 41). We identified an association between the “CD34+ nodular” group and dysmnestic auras suggesting that the CD34+ cells are associated with a pre-ictal activity in the hippocampus. We observed that samples with “CD34+ nodular” cells were linked to type 2, type 3 and to noHS in accordance with the previously reported association of diffuse DNET (which is one possible interpretation of CD34+ cells) with atypical HS (43). We also extended this association of atypical HS with “CD34+ scarce” cells. CD34+ stellate cells are thus associated with the pathogenesis of atypical HS. We found a trend for a better postsurgical outcome associated with CD34+ stellate cells suggesting that they correspond to a focal epileptogenic zone curable by epilepsy surgery. Together, these results reinforce the interest in the CD34 marker for the nosology of HS. They also urge to investigate the role of CD34+ cells in the pathogenesis of MTLE associated to atypical HS.

In conclusion, our data confirms some previously reported clinicopathological correlations of MTLE-HS and opens new perspectives on the heterogeneity of this syndrome – perspectives that may improve the management of those patients (Figure 5). Type 1 is the most frequent, corresponds to the most severe neuronal loss, and is associated with frequent IPI and FS, hypertrophic CA4 neurons and GCL broadening. Type 2 is strongly linked to IPI including FS, and to CD34+ stellate cells. A subgroup of type 1 and a subgroup of type 2 are characterized by GCL duplication, more frequent history of status epilepticus and a higher ratio of patients presenting generalized seizure. Type 3 and the pattern no HS are rare, and associated with rarer IPI, an older age at epilepsy onset and at surgery, and CD34+ stellate cells. MTLE with noHS is associated with more normal MRI and sEEG.

## REFERENCES

1. Barker JM, Galea LA (2008) Repeated estradiol administration alters different aspects of neurogenesis and cell death in the hippocampus of female, but not male, rats. *Neuroscience*.152(4):888-902.
2. Blumcke I, Giencke K, Wardelmann E, Beyenburg S, Kral T, Sarioglu N, Pietsch T, Wolf HK, Schramm J, Elger CE, Wiestler OD (1999) The CD34 epitope is expressed in neoplastic and malformative lesions associated with chronic, focal epilepsies. *Acta Neuropathol*.97(5):481-90.
3. Blumcke I, Kistner I, Clusmann H, Schramm J, Becker AJ, Elger CE, Bien CG, Merschhemke M, Meencke HJ, Lehmann T, Buchfelder M, Weigel D, Buslei R, Stefan H, Pauli E, Hildebrandt M (2009) Towards

- a clinico-pathological classification of granule cell dispersion in human mesial temporal lobe epilepsies. *Acta Neuropathol.*117(5):535-44.
4. Blumcke I, Pauli E, Clusmann H, Schramm J, Becker A, Elger C, Merschhemke M, Meencke HJ, Lehmann T, von Deimling A, Scheiwe C, Zentner J, Volk B, Romstock J, Stefan H, Hildebrandt M (2007) A new clinico-pathological classification system for mesial temporal sclerosis. *Acta Neuropathol.*113(3):235-44.
  5. Blumcke I, Thom M, Aronica E, Armstrong DD, Bartolomei F, Bernasconi A, Bernasconi N, Bien CG, Cendes F, Coras R, Cross JH, Jacques TS, Kahane P, Mathern GW, Miyata H, Moshe SL, Oz B, Ozkara C, Perucca E, Sisodiya S, Wiebe S, Spreafico R (2013) International consensus classification of hippocampal sclerosis in temporal lobe epilepsy: a Task Force report from the ILAE Commission on Diagnostic Methods. *Epilepsia.*54(7):1315-29.
  6. Blumcke I, Thom M, Aronica E, Armstrong DD, Vinters HV, Palmmini A, Jacques TS, Avanzini G, Barkovich AJ, Battaglia G, Becker A, Cepeda C, Cendes F, Colombo N, Crino P, Cross JH, Delalande O, Dubeau F, Duncan J, Guerrini R, Kahane P, Mathern G, Najm I, Ozkara C, Raybaud C, Represa A, Roper SN, Salamon N, Schulze-Bonhage A, Tassi L, Vezzani A, Spreafico R (2011) The clinicopathologic spectrum of focal cortical dysplasias: a consensus classification proposed by an ad hoc Task Force of the ILAE Diagnostic Methods Commission. *Epilepsia.*52(1):158-74.
  7. Blumcke I, Zusratter W, Schewe JC, Suter B, Lie AA, Riederer BM, Meyer B, Schramm J, Elger CE, Wiestler OD (1999) Cellular pathology of hilar neurons in Ammon's horn sclerosis. *J Comp Neurol.*414(4):437-53.
  8. da Costa Neves RS, Jardim AP, Caboclo LO, Lancellotti C, Marinho TF, Hamad AP, Marinho M, Centeno R, Cavalheiro EA, Scorza CA, Targas Yacubian EM (2013) Granule cell dispersion is not a predictor of surgical outcome in temporal lobe epilepsy with mesial temporal sclerosis. *Clin Neuropathol.*32(1):24-30.
  9. de Lanerolle NC, Kim JH, Williamson A, Spencer SS, Zaveri HP, Eid T, Spencer DD (2003) A retrospective analysis of hippocampal pathology in human temporal lobe epilepsy: evidence for distinctive patient subcategories. *Epilepsia.*44(5):677-87.
  10. Deb P, Sharma MC, Tripathi M, Sarat Chandra P, Gupta A, Sarkar C (2006) Expression of CD34 as a novel marker for glioneuronal lesions associated with chronic intractable epilepsy. *Neuropathol Appl Neurobiol.*32(5):461-8.
  11. Deleo F, Garbelli R, Milesi G, Gozzo F, Bramerio M, Villani F, Cardinale F, Tringali G, Spreafico R, Tassi L (2016) Short- and long-term surgical outcomes of temporal lobe epilepsy associated with hippocampal sclerosis: Relationships with neuropathology. *Epilepsia.*57(2):306-15.
  12. Fester L, Ribeiro-Gouveia V, Prange-Kiel J, von Schassen C, Bottner M, Jarry H, Rune GM (2006) Proliferation and apoptosis of hippocampal granule cells require local oestrogen synthesis. *J Neurochem.*97(4):1136-44.
  13. Glover RL, DeNiro LV, Lasala PA, Weidenheim KM, Graber JJ, Boro A (2015) ILAE type 3 hippocampal sclerosis in patients with anti-GAD-related epilepsy. *Neurol Neuroimmunol Neuroinflamm.*2(4):e122.
  14. Harte-Hargrove LC, Maclusky NJ, Scharfman HE (2013) Brain-derived neurotrophic factor-estrogen interactions in the hippocampal mossy fiber pathway: implications for normal brain function and disease. *Neuroscience.*239:46-66.
  15. Hermann BP, Wyler AR, Somes G, Berry AD, 3rd, Dohan FC, Jr. (1992) Pathological status of the mesial temporal lobe predicts memory outcome from left anterior temporal lobectomy. *Neurosurgery.*31(4):652-6; discussion 6-7.
  16. Huse JT, Edgar M, Halliday J, Mikolaenko I, Lavi E, Rosenblum MK (2013) Multinodular and vacuolating neuronal tumors of the cerebrum: 10 cases of a distinctive seizure-associated lesion. *Brain Pathol.*23(5):515-24.
  17. Janszky J, Janszky I, Schulz R, Hoppe M, Behne F, Pannek HW, Ebner A (2005) Temporal lobe epilepsy with hippocampal sclerosis: predictors for long-term surgical outcome. *Brain.*128(Pt 2):395-404.
  18. Japp A, Gielen GH, Becker AJ (2013) Recent aspects of classification and epidemiology of epilepsy-associated tumors. *Epilepsia.*54 Suppl 9:5-11.
  19. Lasarge CL, Danzer SC (2014) Mechanisms regulating neuronal excitability and seizure development following mTOR pathway hyperactivation. *Front Mol Neurosci.*7:18.
  20. Li S, Mattar P, Dixit R, Lawn SO, Wilkinson G, Kinch C, Eisenstat D, Kurrasch DM, Chan JA, Schuurmans C (2014) RAS/ERK signaling controls proneural genetic programs in cortical development and gliomagenesis. *J Neurosci.*34(6):2169-90.
  21. Liu J, Reeves C, Michalak Z, Coppola A, Diehl B, Sisodiya SM, Thom M (2014) Evidence for mTOR pathway activation in a spectrum of epilepsy-associated pathologies. *Acta Neuropathol Commun.*2:71.
  22. Louis DN, Ohgaki H, Wiestler OD, Cavenee WK (2016) WHO classification of tumours of the central nervous system, Revised. 4th update Edition, International Agency for Research On Cancer: Lyon.

23. Marucci G, Martinoni M, Giulioni M (2013) Relationship between focal cortical dysplasia and epilepsy-associated low-grade tumors: an immunohistochemical study. *APMIS*.121(1):22-9.
24. Mathern GW, Kuhlman PA, Mendoza D, Pretorius JK (1997) Human fascia dentata anatomy and hippocampal neuron densities differ depending on the epileptic syndrome and age at first seizure. *J Neuropathol Exp Neurol*.56(2):199-212.
25. Mathon B, Bielle F, Samson S, Plaisant O, Dupont S, Bertrand A, Miles R, Nguyen-Michel VH, Lambrecq V, Calderon-Garciduenas AL, Duyckaerts C, Carpentier A, Baulac M, Cornu P, Adam C, Clemenceau S, Navarro V (2017) Predictive factors of long-term outcomes of surgery for mesial temporal lobe epilepsy associated with hippocampal sclerosis. *Epilepsia*.
26. Mirzaa GM, Campbell CD, Solovieff N, Goold CP, Jansen LA, Menon S, Timms AE, Conti V, Biag JD, Olds C, Boyle EA, Collins S, Ishak G, Poliachik SL, Girisha KM, Yeung KS, Chung BH, Rahikkala E, Gunter SA, McDaniel SS, Macmurdo CF, Bernstein JA, Martin B, Leary RJ, Mahan S, Liu S, Weaver M, Dorschner MO, Jhangiani S, Muzny DM, Boerwinkle E, Gibbs RA, Lupski JR, Shendure J, Saneto RP, Novotny EJ, Wilson CJ, Sellers WR, Morrissey MP, Hevner RF, Ojemann JG, Guerrini R, Murphy LO, Winckler W, Dobyns WB (2016) Association of MTOR Mutations With Developmental Brain Disorders, Including Megalencephaly, Focal Cortical Dysplasia, and Pigmentary Mosaicism. *JAMA Neurol*.73(7):836-45.
27. Na M, Ge H, Shi C, Shen H, Wang Y, Pu S, Liu L, Wang H, Xie C, Zhu M, Wang J, Shi C, Lin Z (2015) Long-term seizure outcome for international consensus classification of hippocampal sclerosis: a survival analysis. *Seizure*.25:141-6.
28. Nagaishi M, Yokoo H, Nobusawa S, Fujii Y, Sugiura Y, Suzuki R, Tanaka Y, Suzuki K, Hyodo A (2015) Localized overexpression of alpha-internexin within nodules in multinodular and vacuolating neuronal tumors. *Neuropathology*.35(6):561-8.
29. Pasquier B, Peoc HM, Fabre-Bocquentin B, Bensaadi L, Pasquier D, Hoffmann D, Kahane P, Tassi L, Le Bas JF, Benabid AL (2002) Surgical pathology of drug-resistant partial epilepsy. A 10-year-experience with a series of 327 consecutive resections. *Epileptic Disord*.4(2):99-119.
30. Ryufuku M, Toyoshima Y, Kitaura H, Zheng Y, Fu YJ, Miyahara H, Murakami H, Masuda H, Kameyama S, Takahashi H, Kakita A (2011) Hypertrophy of hippocampal end folium neurons in patients with mesial temporal lobe epilepsy. *Neuropathology*.31(5):476-85.
31. Scharfman H, Goodman J, Macleod A, Phani S, Antonelli C, Croll S (2005) Increased neurogenesis and the ectopic granule cells after intrahippocampal BDNF infusion in adult rats. *Exp Neurol*.192(2):348-56.
32. Semah F, Picot MC, Adam C, Broglin D, Arzimanoglou A, Bazin B, Cavalcanti D, Baulac M (1998) Is the underlying cause of epilepsy a major prognostic factor for recurrence? *Neurology*.51(5):1256-62.
33. Sha LZ, Xing XL, Zhang D, Yao Y, Dou WC, Jin LR, Wu LW, Xu Q (2012) Mapping the spatio-temporal pattern of the mammalian target of rapamycin (mTOR) activation in temporal lobe epilepsy. *PLoS One*.7(6):e39152.
34. Shima A, Nitta N, Suzuki F, Laharie AM, Nozaki K, Depaulis A (2015) Activation of mTOR signaling pathway is secondary to neuronal excitability in a mouse model of mesio-temporal lobe epilepsy. *Eur J Neurosci*.41(7):976-88.
35. Tanapat P, Hastings NB, Gould E (2005) Ovarian steroids influence cell proliferation in the dentate gyrus of the adult female rat in a dose- and time-dependent manner. *J Comp Neurol*.481(3):252-65.
36. Tanapat P, Hastings NB, Reeves AJ, Gould E (1999) Estrogen stimulates a transient increase in the number of new neurons in the dentate gyrus of the adult female rat. *J Neurosci*.19(14):5792-801.
37. Tezer FI, Xasiyev F, Soylemezoglu F, Bilginer B, Oguz KK, Saygi S (2016) Clinical and electrophysiological findings in mesial temporal lobe epilepsy with hippocampal sclerosis, based on the recent histopathological classifications. *Epilepsy Res*.127:50-4.
38. Thom M (2014) Review: Hippocampal sclerosis in epilepsy: a neuropathology review. *Neuropathol Appl Neurobiol*.40(5):520-43.
39. Thom M, D'Arrigo C, Scaravilli F (1999) Hippocampal sclerosis with hypertrophy of end folium pyramidal cells. *Acta Neuropathol*.98(1):107-10.
40. Thom M, Liagkouras I, Elliot KJ, Martinian L, Harkness W, McEvoy A, Caboclo LO, Sisodiya SM (2010) Reliability of patterns of hippocampal sclerosis as predictors of postsurgical outcome. *Epilepsia*.51(9):1801-8.
41. Thom M, Liu J, Bongaarts A, Reinten RJ, Paradiso B, Jager HR, Reeves C, Somani A, An S, Marsdon D, McEvoy A, Miserocchi A, Thorne L, Newman F, Bucur S, Honavar M, Jacques T, Aronica E (2017) Multinodular and vacuolating neuronal tumors in epilepsy: dysplasia or neoplasia? *Brain Pathol*.
42. Thom M, Sisodiya SM, Beckett A, Martinian L, Lin WR, Harkness W, Mitchell TN, Craig J, Duncan J, Scaravilli F (2002) Cytoarchitectural abnormalities in hippocampal sclerosis. *J Neuropathol Exp Neurol*.61(6):510-9.
43. Thom M, Toma A, An S, Martinian L, Hadjivassiliou G, Ratilal B, Dean A, McEvoy A, Sisodiya SM, Brandner S (2011) One hundred and one dysembryoplastic neuroepithelial tumors: an adult epilepsy series with

immunohistochemical, molecular genetic, and clinical correlations and a review of the literature. *J Neuropathol Exp Neurol*.70(10):859-78.

44. Vilar M, Mira H (2016) Regulation of Neurogenesis by Neurotrophins during Adulthood: Expected and Unexpected Roles. *Front Neurosci*.10:26.

45. Wieser HG, Epilepsy ICoNo (2004) ILAE Commission Report. Mesial temporal lobe epilepsy with hippocampal sclerosis. *Epilepsia*.45(6):695-714.

46. Willment KC, Golby A (2013) Hemispheric lateralization interrupted: material-specific memory deficits in temporal lobe epilepsy. *Front Hum Neurosci*.7:546.

47. Wyler AR, Dohan FC, Schweitzer JB, Berry AD (1992) A grading system for mesial temporal pathology (hippocampal sclerosis) from anterior temporal lobectomy. *J Epilepsy* 5:220-25.

## FIGURES LEGEND

### Figure 1. CD34+ cells are associated with rarer patterns of hippocampal sclerosis

a-d,i-j. A CD34+ nodular case. CD34 immunopositive/CD34+ stellate cells formed a nodule (solid arrowheads in a-b). Nestin immunolabeling showed a frequent extravascular stellate pattern in the area of the CD34+ nodule (solid arrowhead in c) whereas Vimentin immunolabeling showed no extravascular immunolabeling (d). e-h,k-l. A CD34+ scarce case. e. An isolated CD34+ extravascular stellate cell is observed (open arrowheads in e,f). Nestin immunolabeling showed a scant stellate extravascular pattern in the area of the CD34+ stellate cell (open arrowhead in g) whereas Vimentin immunolabeling showed no extravascular immunolabeling (h). Double immunolabelings showed the co-expression in stellate cells of Nestin (*brown*) and CD34 (*red*) (i), and SOX2 (*pink*) and CD34 (*brown*) (j) in a CD34+ nodular case. Double immunolabelings showed the co-expression in stellate cells of Nestin (*brown*) and CD34 (*red*) (k, higher magnification in insert), and of SOX2 (*pink*) and CD34 (*brown*) (l) in a CD34+ scarce case. m-p. Distribution of CD34 immunolabeling (CD34 negative in *black*, CD34+ scarce in *orange* and CD34+ nodular in *green*) for type 1 (m), type 2 (n), type 3 (o), the pattern noHS (p). q-s. A CD34+ nodular case with BRAF V600E immunopositive neurons. q. A moderate immunolabeling of scarce cells by P53 (solid arrowheads). The BRAF V600E immunolabeling is positive in neurons (solid arrowheads in r,s). t. A CD34+ scarce case with BRAF V600E+ neurons (open arrowhead). Scale bars: a,e 400  $\mu$  m; b-d,f-h 100  $\mu$  m; i-l,t 50  $\mu$  m; q,r 200  $\mu$  m; s 20  $\mu$  m.

### Figure 2. Classification of CD34+ hippocampal sclerosis according to BRAF V600E and INA status.

a,c,e,g-i. A case of “BRAF V600E+ HS” with BRAF V600E positive neurons. b,d,f,j-l. A case of hippocampal MVNT. a,b. CD34 immunolabeling showed a nodular pattern of CD34 positive stellate cells (solid arrowheads).



c,d. NeuN immunolabeling showed a neuronal loss that is predominant in CA4 (solid arrowheads) corresponding to HS ILAE type 3. e. Absence of INA positive abnormal neurons. f. Presence of numerous abnormal INA+ neurons (solid arrowheads).

g-i. Absence of abnormal neurons according to NeuN, ELAVL2 and INA immunolabelings in the white matter of CA2 (open arrowheads) in a BRAF V600E+ HS. j-l. Presence of Neun Negative, ELAVL2 positive, INA positive abnormal neurons (solid arrowheads) in the white matter of CA2 in a MVNT.

Scale bars: a-f 2.5mm; g-l 200  $\mu$  m . Abbreviations: INA, internexin alpha; MVNT: multinodular and vacuolating neuronal tumour.

### **Figure 3. Radiological features of BRAF V600E+ hippocampal sclerosis and hippocampal MVNT.**

a-b. BRAF V600E+ hippocampal sclerosis. Coronal T2 sequence showing discrete atrophy, loss of digitation and T2 hyperintensity of the right hippocampus (vertical arrows). c-e. Hippocampal MVNT. Coronal T2 (c), FLAIR (d) and T1 (e) sequences show discrete atrophy of left internal temporal structures (vertical arrows), associated with extensive T2 and FLAIR hyperintensities involving the hippocampus, parahippocampal gyrus, fusiform gyrus and part of the inferior temporal gyrus (oblique arrows). A pseudocyst (arrowheads) is visible within the fusiform gyrus, hyperintense on T2 and hypointense on T1 and FLAIR images.

### **Figure 4. Prognostic value of histopathological lesions of hippocampal sclerosis in the postsurgical outcome**

Kaplan-Meier plots are shown for Engel I and Engel Ia classes of postsurgical outcome: the ratio of patients fulfilling the criteria of Engel I (a,c,e) and Engel Ia (b,d,f) classes are depicted during the postsurgical follow-up (time in years). a,b. In the type 1, presence of CA4 hypertrophic neurons (*blue curve*, n=89) had a significant worse prognosis than absence of CA4 hypertrophic neurons (*purple curve*, n=83). c-d. in the types 1 and 2, absence of broadening of the dentate gyrus granule cell layer (*purple curve*, n=44), their dispersion (*blue curve*, n=137) and their duplication (*black curve*, n=24) had no prognostic value. e-f. Presence of CD34+ stellate cells (*blue curve*, n=43) has no prognostic value for the Engel I class but showed a trend for a better prognosis than the absence of CD34+ stellate cells (*purple curve*, n=170) for the Engel Ia class.

### **Figure 5. Clinicopathological correlates of ILAE types of HS and of their subgroups**

Distinctive clinicopathological features of the four ILAE types of HS are summarized. CA4 hypertrophic neurons are more frequent in type 1 and are associated with worse postsurgical prognosis. GCL duplication identified a subgroup of type 1 and a subgroup of type 2. It is associated with a higher prevalence of presurgical status epilepticus and/or generalized seizures. CD34+ stellate cells were more frequently observed in the rarest ILAE types: 2, 3, noHS. The “CD34+ scarce” pattern was associated with higher prevalence of normal MRI and stereo-encephalographic studies. The “CD34+ nodular” pattern was associated with dysmnestic auras.

### **SUPPLEMENTARY FIGURES LEGEND**

#### **Supplemental Figure 1. Clinical features of mesial temporal lobe epilepsy – hippocampal sclerosis**

a. A flowchart shows the steps for the inclusion of samples in the study according to the indicated criteria. b. Distribution of the age of epilepsy onset in the patient population. c. Distribution of the duration of epilepsy. d. Epilepsy duration plotted against the date of surgery. e. Neuronal loss in the CA2 region of type 1 was positively correlated with age at the first FS (n=69, p=0.0035, rho=0.36).

#### **Supplemental Figure 2. Neuronal loss evaluation in the ILAE types of hippocampal sclerosis**

a-h. NeuN immunolabeling in CA1 (a-d) and CA4 (e-h) in hippocampal sclerosis of type 1 (a,e), type 2 (b,f), type 3 (c,g) and in the pattern noHS, gliosis only (d,h). i. Percentage of neuronal loss in CA1, CA2, CA3, CA4 is shown as box and whisker plots for type 1 (blue), type 2 (red), type 3 (green) and type noHS, gliosis only (pink). By definition there is no neuronal loss in the pattern noHS, gliosis only. Although the ILAE classification is based on the predominance of neuronal loss in either CA1 and/or CA4 fields, we noticed that some neuronal loss was also present in the GCL and in the CA2 and CA3 regions. Neuronal loss in CA2 was significantly higher in type 1 than in type 2 ( $p < 10^{-4}$ ). It was higher in type 2 than in type 3 ( $p = 7 \times 10^{-4}$ ) and than in noHS ( $p = 10^{-4}$ ). Neuronal loss in CA3 field was significantly higher in type 1 than in type 2 ( $p < 10^{-4}$ ) and higher in type 2 than in noHS samples ( $p = 2 \times 10^{-4}$ ). Loss of dentate granule cells was significantly higher in type 1 than in type 2 ( $p = 0.002$ ) and higher in type 2 than in noHS ( $p = 0.007$ ). Scale bars: a-h 200  $\mu$  m.

#### **Supplemental Figure 3. Histopathological aspects of hypertrophic CA4 neurons and of broadening of the granule cell layer of the dentate gyrus.**

a-c. Hematoxylin eosin, 400X. Normal CA4 neurons (a), hypertrophic CA4 neurons (b,c). d. The longer axis ( $\mu$ m) of the nucleus of CA4 pyramidal neurons was significantly increased in hypertrophic CA4 neurons of HS

(20.8  $\mu\text{m} \pm 3.2$  red) compared to CA4 neurons of a control hippocampus (14.5  $\mu\text{m} \pm 2.0$  blue,  $p < 0.0001$ ). e. The longer axis ( $\mu\text{m}$ ) of the cell soma of CA4 pyramidal neurons was significantly increased in hypertrophic CA4 neurons of HS (52.6  $\mu\text{m} \pm 14$  red) compared to CA4 neurons of a control hippocampus (27.8  $\mu\text{m} \pm 7.9$  blue,  $p < 0.0001$ ). f. The ratio between the longer axis of the nucleus and the longer axis of the cell soma of CA4 pyramidal neurons was significantly decreased in hypertrophic CA4 neurons of HS (0.42  $\pm 0.1$  red) compared to CA4 neurons of a control hippocampus (0.55  $\mu\text{m} \pm 0.1$  blue,  $p < 0.0001$ ). g-i. NeuN immunolabeling, 200X. Normal granule cell layer/GCL of the dentate gyrus (g), dispersion of the GCL (h), duplication of the GCL (i). Scale bars: a-c 100  $\mu\text{m}$ , d-e 100  $\mu\text{m}$ .

#### **Supplemental Figure 4. Expression of OLIG2 by CD34+ stellate cells**

a-c. Co-expression of OLIG2 (pink) and CD34 (brown) by CD34+ stellate cells in a CD34+ nodular case.

Scale bars: a-c 50  $\mu\text{m}$ .

#### **Supplemental Figure 5. Histopathological aspect of hippocampal MVNT**

The parahippocampic white matter (a,c) and the alveus (b,d) harboured nodules (black arrowheads in a,b) containing neuropile, vacuolated neurons and vacuoles (white arrowheads in c,d).

Scale bars: a-b: 1mm, c-d: 100  $\mu\text{m}$ .

	n (%)
<b>Clinical features</b>	
Male	121 (49)
IPI	191/246 (78)
IPI age (years)	2.0 ±3.1
Febrile seizure	137/246 (56)
Family history of epilepsy	50/175 (29)
Age of onset of epilepsy (years)	12.3 ±9.3
Epilepsy duration before surgery (years)	26.0 ±11.7
Right side of hippocampectomy	119 (48)
Number of seizures per month	19 ±30
Number of antiepileptic drugs	1.7 ±0.8
Status epilepticus	19/211 (9)
Abnormal hippocampus on MRI	219/227 (96)
Cognitive impairment:	
-None	17/233 (7)
-Verbal	88/233 (38)
-Non verbal	48/233 (21)
-Global	80/233 (34)
<b>Histological features</b>	
CA1 neuronal loss	81% ±19
CA2 neuronal loss	39% ±19
CA3 neuronal loss	58% ±24
CA4 neuronal loss	62% ±22
GCL neuronal loss	25% ±23
GCL pattern normal	56/239 (23)
GCL pattern dispersion	158/239 (66)
GCL pattern duplication	25/239 (10)
Hypertrophic CA4 neurons	106 (43)
Dysplasia	1 (0,4)

**Table 1. Clinico-pathological features in 247 patients with MTLE.**

n was precised if it was inferior to the total number of patients (247).

	ILAE type 1 n=186	ILAE type 2 n=47	ILAE type 3 n=7	ILAE type noHS n=7	p value
<b>Clinical features</b>					
IPI	144 (77%)	42 (89%)*	3/7 (43%)	2/6 (33%)*	<b>0.001</b>
Febrile seizure	104 (56%)	32 (68%)	0 (0%)	1/5 (17%)*	<b>6x10<sup>-4</sup></b>
sEEG	14/172 (8%)	1 (2%)	1 (14%)	5 (71%)*	<b>6x10<sup>-5</sup></b>
Abnormal hippocampus on MRI	168/170 (99%)	43/43 (100%)	6 (86%)	2 (29%)*	<b>7x10<sup>-8</sup></b>
<b>Histological features</b>					
CA1 neuronal loss (%)	85 ±8	84 ±9	10 ±17	0 ±0	<10 <sup>-4</sup>
CA2 neuronal loss (%)	<b>44 ±18*</b>	<b>30 ±16*</b>	3 ±8	0 ±0	<10 <sup>-4</sup>
CA3 neuronal loss (%)	<b>69 ±16*</b>	<b>34 ±18*</b>	35 ±34	0 ±0	<10 <sup>-4</sup>
CA4 neuronal loss (%)	<b>72 ±12*</b>	32 ±9	47 ±23	0 ±0	<10 <sup>-4</sup>
GCL neuronal loss (%)	<b>29 ±23*</b>	<b>18±21*</b>	17±29	0 ±0	<10 <sup>-4</sup>
Hypertrophic CA4 neurons	<b>98 (57%)*</b>	7 (15%)	1 (14%)	0	<b>1x10<sup>-7</sup></b>

**Table 2. Clinical and pathological features associated with ILAE types**

n was precised if it was inferior to the total number of each group

Abbreviations: sEEG, stereo-electroencephalography.

	Normal GCL thickness n=56		GCL broadening n=183		Statistical tests Norm. vs Abnorm. p value	Dispersion of GCL n=158		Duplication of GCL n=25		Statistical tests Norm. vs Disp. and Dup. p value
<b>Clinical features</b>										
Sex (male)	34	(61%)	83	(45%)	<b>0.044*</b>	73	(46%)	10	(40%)	0.11
Intracranial infection	12/55	(22%)	16	(9%)	<b>0.008*</b>	<b>11*</b>	<b>(7%)</b>	5	(20%)	<b>0.005*</b>
Gen. seizure	<b>40</b>	<b>(71%)</b>	131/182	(72%)	0.94	<b>107/157</b>	<b>(68%)</b>	<b>24*</b>	<b>(96%)</b>	<b>0.02*</b>
Stat. epilepticus	<b>1*/48</b>	<b>(2%)</b>	17/156	(11%)	0.08	13/136	(10%)	<b>4*/20</b>	<b>(20%)</b>	<b>0.04*</b>
Abnormal hippocampus on MRI	<b>45*/50</b>	<b>(90%)</b>	<b>166/169*</b>	<b>(98%)</b>	<b>0.02*</b>	144/147	(98%)	22/22	(100%)	<b>0.04*</b>
<b>Histological features</b>										
ILAE type 1	<b>34</b>	<b>(61%)<sup>§</sup></b>	<b>144</b>	<b>(79%)<sup>§</sup></b>	<b>0.01<sup>§</sup></b>	<b>125</b>	<b>(79%)<sup>§</sup></b>	<b>19</b>	<b>(76%)</b>	<b>0.04*</b>
ILAE type 2	<b>14</b>	<b>(25%)</b>	<b>33</b>	<b>(18%)</b>		27	(17%)	6	(24%)	
ILAE type 3	3	(5%)	4	(2%)		4	(3%)	0	(0%)	
ILAE noHS	<b>5</b>	<b>(9%)<sup>§</sup></b>	<b>2</b>	<b>(1%)<sup>§</sup></b>		<b>2</b>	<b>(1%)<sup>§</sup></b>	<b>0</b>	<b>(0%)</b>	
CA1 neur. loss (%)	76 ±27		82 ±16		0.74	81 ±17		86 ±7.1		0.48
CA2 neur. loss (%)	35 ±20		40 ±19		0.13	<b>41* ±20</b>		33 ±13		<b>0.045*</b>
CA3 neur. loss (%)	51 ±26		<b>61* ±23</b>		<b>0.02*</b>	<b>63* ±24</b>		51 ±19		<b>0.003*</b>
CA4 neur. loss (%)	<b>53* ±25</b>		<b>64* ±20</b>		<b>0.003*</b>	64 ±21		65 ±19		<b>0.011*</b>
GCL neur. loss (%)	27 ±30		25 ±21		0.63	24 ±21 (n=157)		27 ±21		0.74

**Table 3. Clinico-pathological features associated with granule cell layer changes.**

n is precised if it was inferior to the total number of each group

<sup>§</sup>: GCL broadening is significantly more frequent in type 1 compared to type noHS (p=0.005). GCL dispersion is significantly more frequent in type 1 compared to noHS (p=0.008).

Abbreviations: GCL, Granule Cell Layer; Gen. seizure, generalized seizure; neuron. loss, neuronal loss; Stat. epilepticus, status epilepticus.

	CD34 negative n=196	CD34+ stellate cells n=43	p value	“CD34+ scarce” stellate cells n=35	“CD34+ nodular” stellate cells n=8	p value
<b>Presurgical clinical features</b>						
Fetal distress	6/189 (7%)	2/41 (5%)	0.63	0/33 (0%)	<b>2*</b> (25%)	<b>0.02*</b>
Dysmnestic aura	<b>59/176 (34%)</b>	<b>19/36 (53%)</b>	<b>0.037*</b>	12/28 (43%)	<b>7*</b> (88%)	<b>0.006*</b>
sEEG	<b>13<sup>+</sup></b> (7%)	<b>8<sup>+</sup></b> (19%)	<b>0.031*</b>	<b>7<sup>+</sup></b> (20%)	1 (13%)	<b>0.034*</b>
Abnormal hippocampus on MRI	178/182 (98%)	<b>34/38 (89%)</b>	<b>0.032*</b>	<b>26/30* (87%)</b>	8 (100%)	<b>0.021*</b>
<b>Histological features</b>						
ILAE type 1	<b>156<sup>&amp;</sup></b> (80%)	<b>23<sup>&amp;</sup></b> (53%)	<b>0.0002*<sup>§</sup></b>	<b>22/35<sup>§</sup></b> (63%)	<b>1/8<sup>§</sup></b> (12%)	<b>3x10<sup>-6*</sup><sup>§</sup></b>
ILAE type 2	<b>34<sup>&amp;</sup></b> (17%)	<b>12<sup>&amp;</sup></b> (28%)		9/35 (26%)	<b>3/8<sup>§</sup></b> (38%)	
ILAE type 3	4 (2%)	3 (7%)		0/35 (0%)	<b>3/8<sup>§</sup></b> (38%)	
ILAE noHS	<b>2<sup>&amp;</sup></b> (1%)	<b>5<sup>&amp;</sup></b> (12%)		<b>4/35<sup>§</sup></b> (11%)	<b>1/8<sup>§</sup></b> (12%)	
CA1 neuronal loss(%)	83 ±16	70 ±30	<b>&lt;10<sup>-4*</sup></b>	74 ±28	<b>45* ±42</b>	<b>0.002*</b>
CA2 neuronal loss (%)	<b>40* ±19 (153)</b>	29 ±22 (35)	<b>0.005*</b>	31 ±22 (29)	<b>20* ±18 (6)</b>	<b>0.044*</b>
CA3 neuronal loss(%)	60 ±23 (134)	49 ±31 (33)	0.03	51 ±30 (28)	40 ±37 (5)	0.21
CA4 neuronal loss(%)	<b>64* ±21</b>	48 ±27	<b>&lt;10<sup>-4*</sup></b>	50 ±27	43 ±29	<b>0.003*</b>
GCL neuronal loss(%)	27 ±24 (188)	17 ±22 (42)	<b>0.01*</b>	19 ±22	9 ±17	<b>0.008*</b>

**Table 4. Clinical and pathological features of hippocampal sclerosis according to CD34 status**

n is precised if it was inferior to the total number of each group.

<sup>+</sup>: the “CD34+ scarce” group and the “CD34+” group were significantly associated to sEEG compared to “CD34 negative” group.

<sup>§</sup>: type 3 was excluded from statistical test because of a too small number of cases.

<sup>&</sup>: CD34+ stellate cells were significantly more frequent in type 2 and in noHS than in type 1.

<sup>§</sup>: “CD34+ scarce” stellate cells were significantly associated with noHS compared to type 1 (p=0.004). The “CD34+ nodular” group was significantly associated with type 2 (p=0.023), type 3 (p=0.0002) and noHS (p=0.0004) compared to type 1.

Abbreviations, sEEG: stereo-electroencephalography

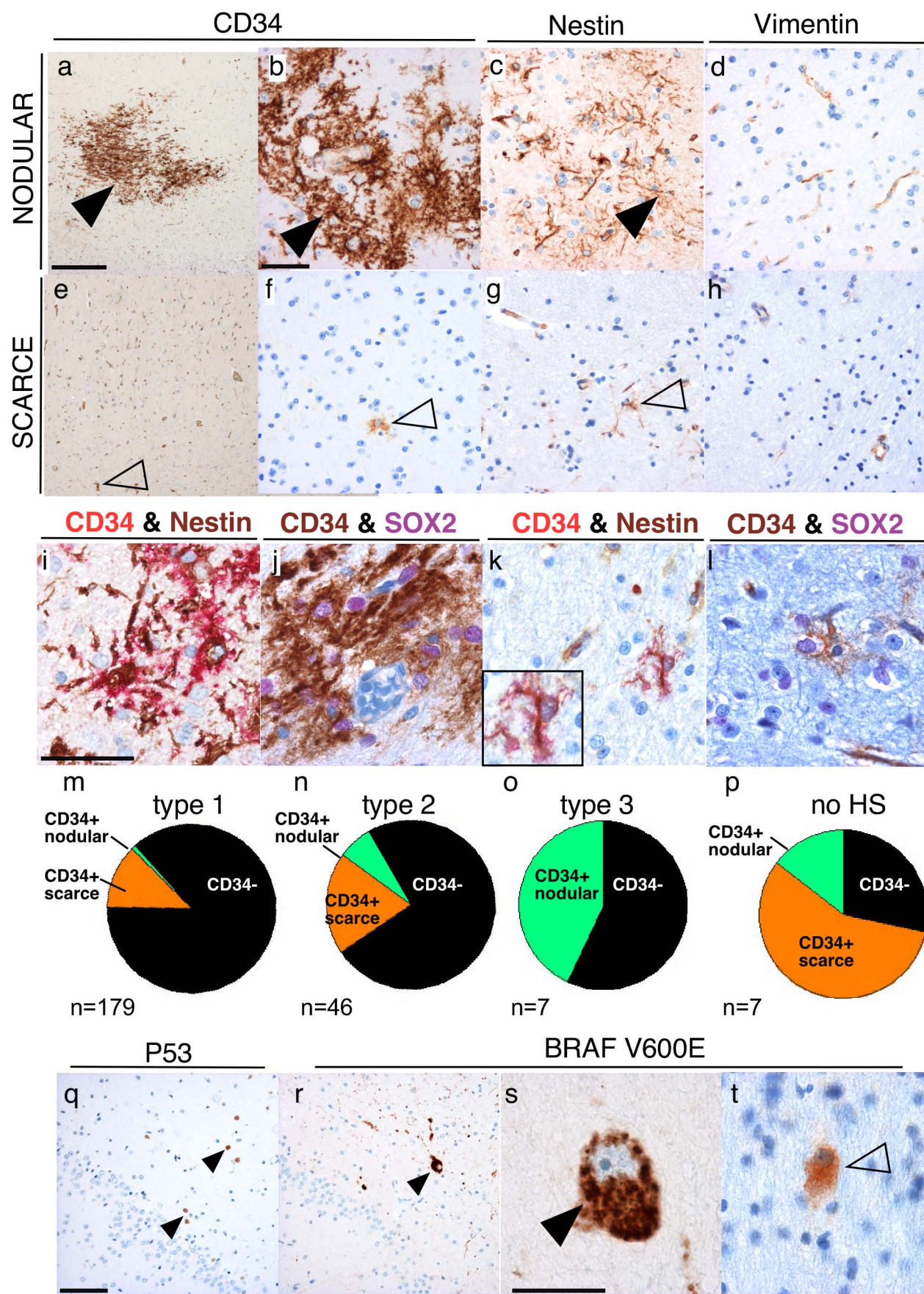


**Figure 1**

This article is protected by copyright. All rights reserved.



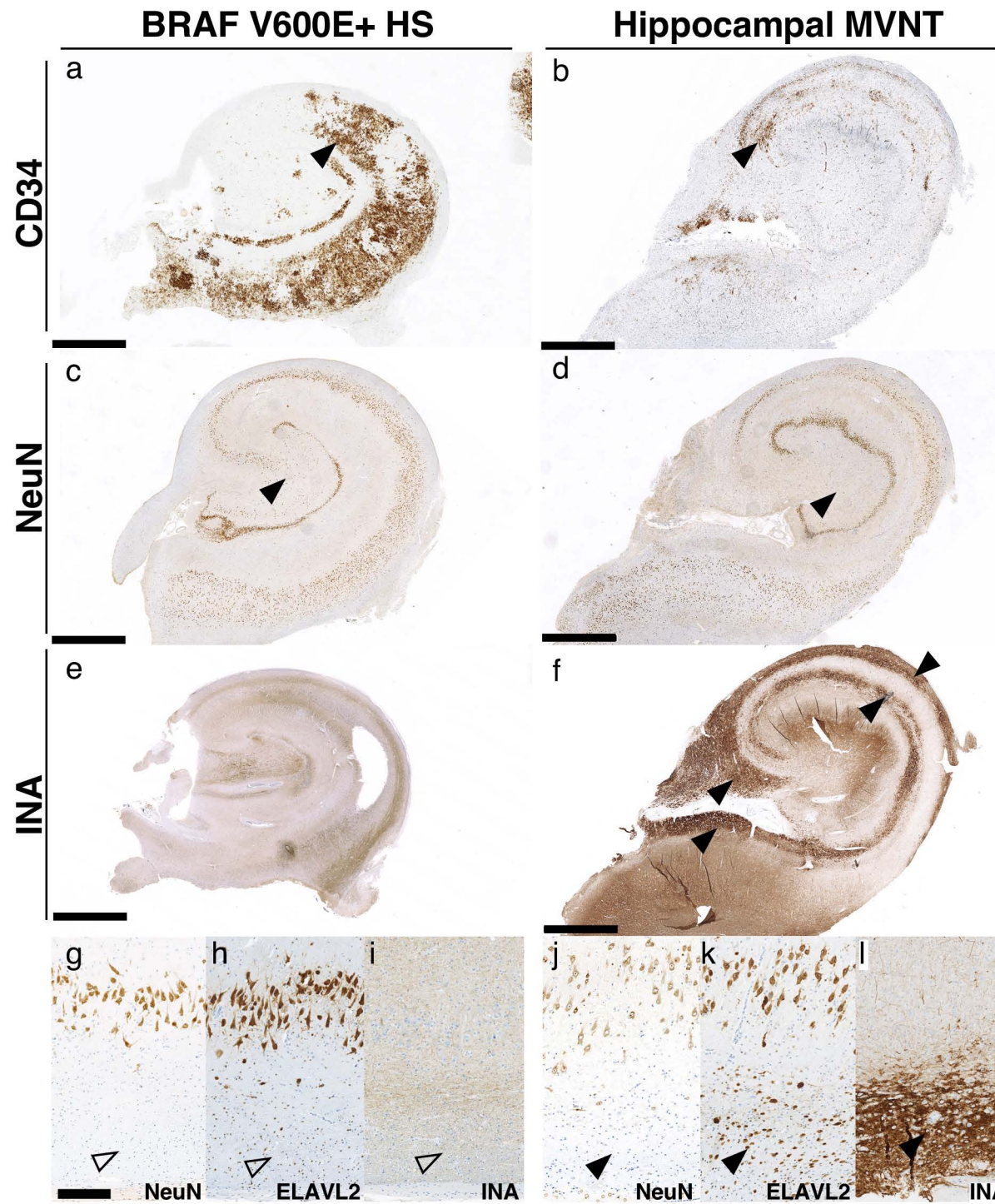


**Figure 2**

This article is protected by copyright. All rights reserved.

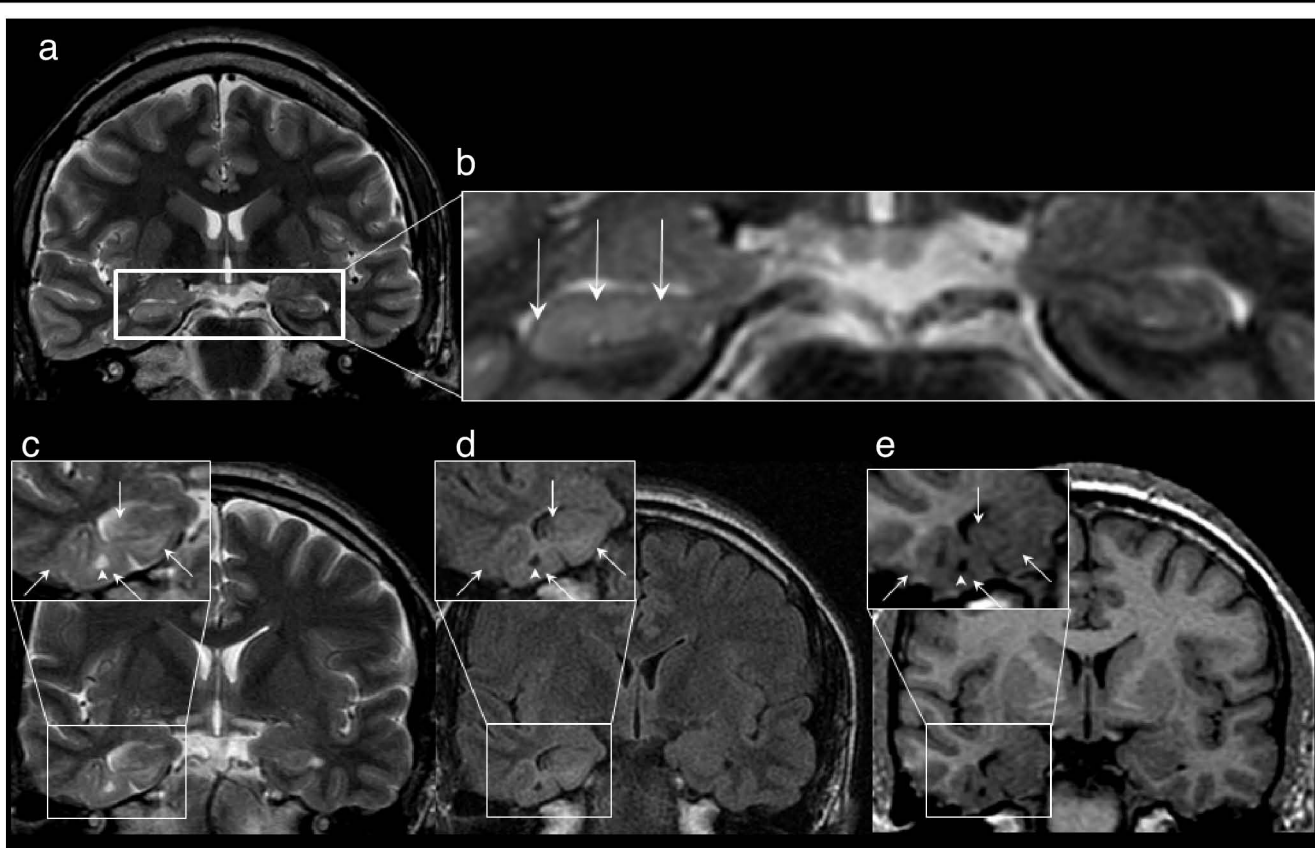


**Figure 3**

This article is protected by copyright. All rights reserved.

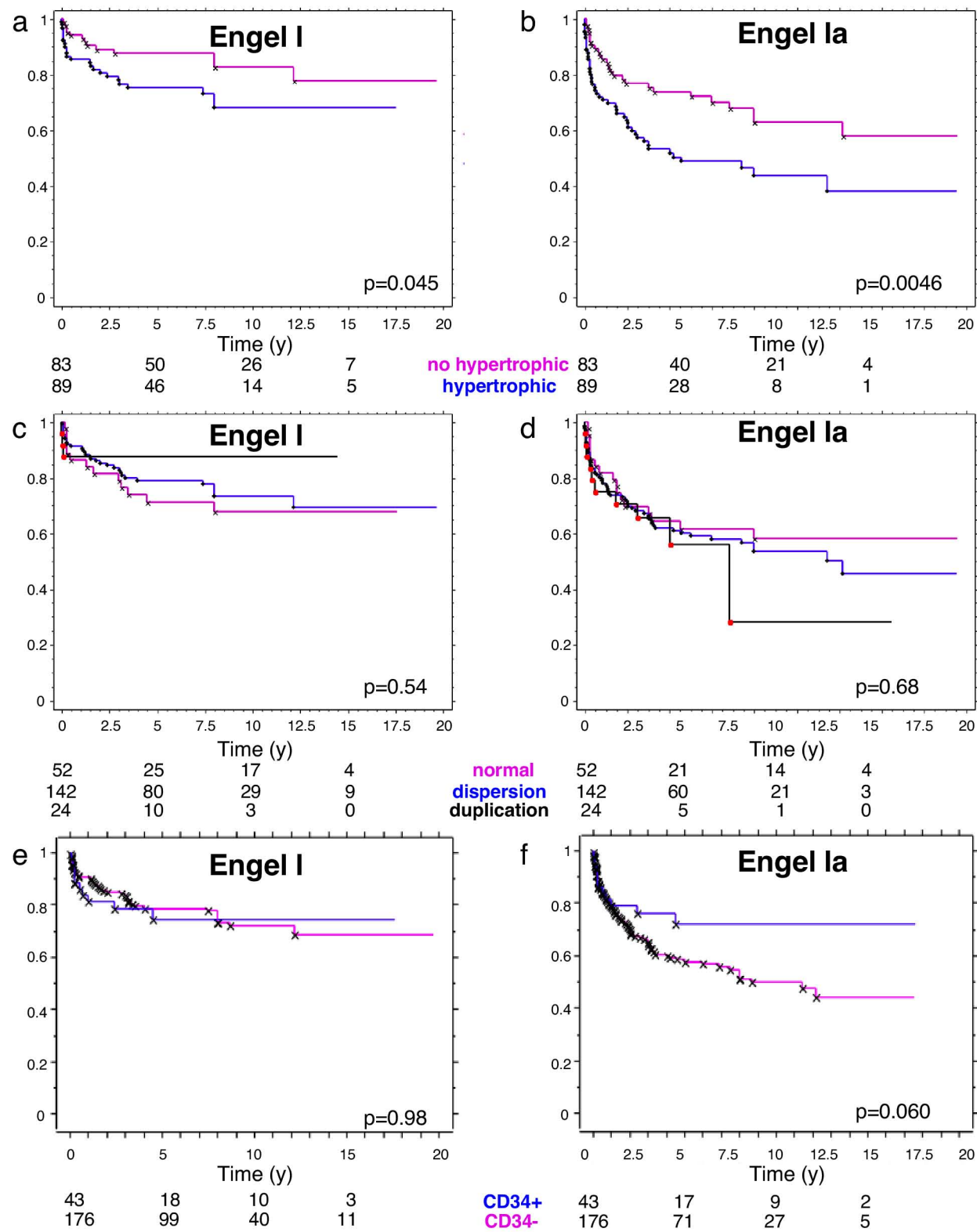


**Figure 4**

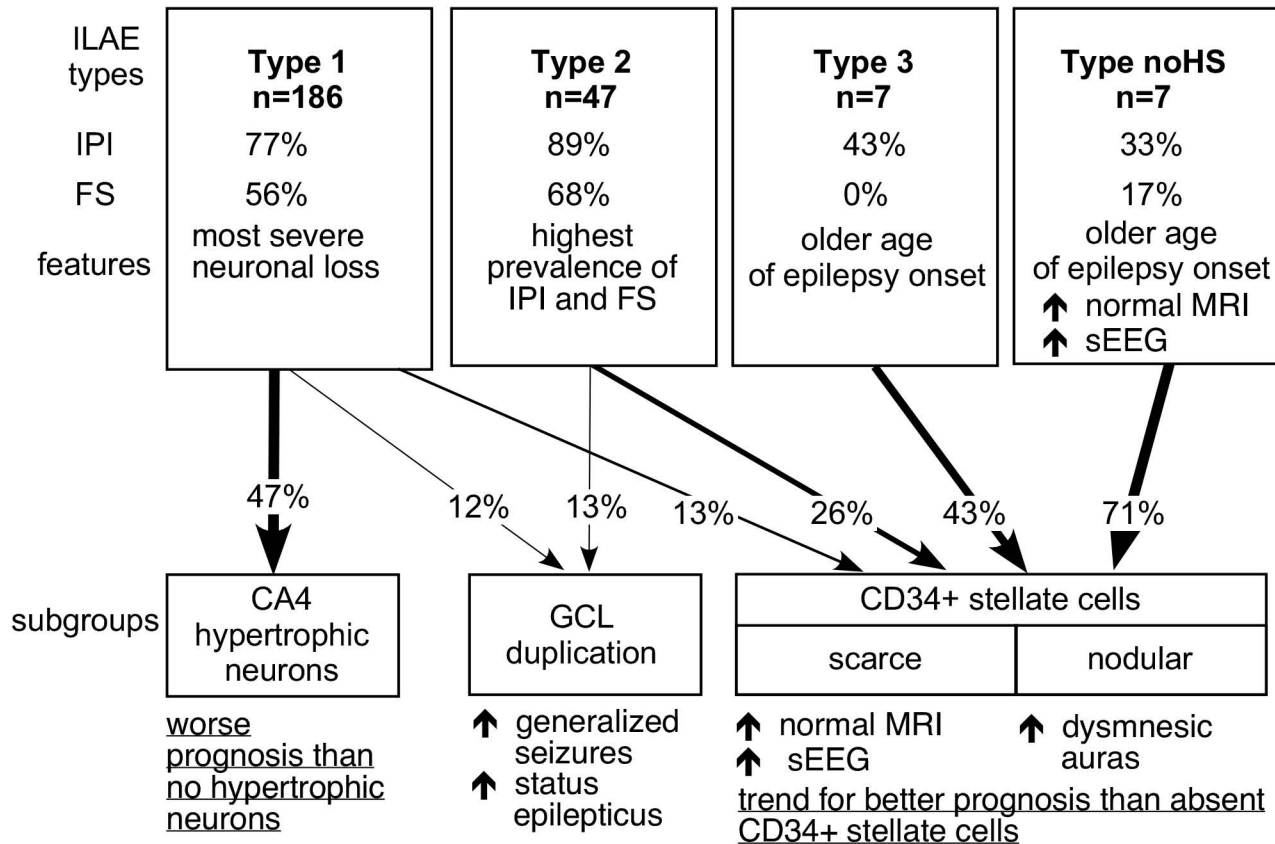


# Figure 5

This article is protected by copyright. All rights reserved.